Review

Core-collapse supernova explosion theory

https://doi.org/10.1038/s41586-020-03059-w

Received: 20 July 2020

Accepted: 29 September 2020

Published online: 6 January 2021

Check for updates

A. Burrows[1]✉ & D. Vartanyan[2]

Most supernova explosions accompany the death of a massive star. These explosions give birth to neutron stars and black holes, and eject solar masses of heavy elements. However, determining the mechanism of explosion has been a half-century journey of great numerical and physical complexity. Here we present the status of this theoretical quest and the physics and astrophysics upon which its resolution seems to depend. The delayed neutrino-heating mechanism is emerging as the key driver of supernova explosions, but there remain many issues to address, such as the chaos of the involved dynamics.

Stars are born, they live and they die. Many terminate their thermonuclear lives after billions of years of cooking light elements into heavier elements by ejecting their outer hydrogen-rich envelopes over perhaps hundreds of years. In the process, they give birth to compact white dwarf stars that are half as massive as the Sun but a hundred times smaller. Such dense remnants cool off over billions of years like dying embers plucked from a fire. A subset of these white dwarfs in binary stellar systems will later (perhaps hundreds of millions of years later) ignite in spectacular thermonuclear explosions. Owing to their brightness from across the Universe, many of these so-called type Ia supernovae are used to take its measure.

However, some stars—those more massive than about $8M_{\odot}$ ($M_{\odot}$, solar mass)—die violently in supernova explosions that inject freshly synthesized elements, progressively enriching the interstellar medium with these products of existence. They too leave behind remnants: neutron stars and black holes. The former could become radio pulsars, are only the size of a city and have masses of about $1.5M_{\odot}$ on average. The latter are perhaps a few to ten times more massive than a neutron star, but even more compact and more exotic.

The supernova explosions of these massive stars, the so-called core-collapse supernovae, have been studied theoretically for more than half a century and investigated observationally even longer. Yet, the mechanism of their explosion has only recently come into sharp focus. A white dwarf is birthed in these stars as well, but before their outer envelope can be ejected, this white dwarf reaches the Chandrasekhar mass[1], near about $1.5M_{\odot}$, which is gravitationally unstable to implosion. After a life of about 10–40 million years, the dense core of this star implodes within less than a second to neutron-star densities, at which point it rebounds like a spherical piston, generating a shock wave in the outer imploding core. The temperatures and densities achieved lead to the copious generation of neutrinos, so the treatment of the neutrinos and their interaction with dense matter are of great import. This 'bounce' shock wave could have been the supernova, but in all credible models this shock wave stalls into accretion, halting its outward progress. This is an unsatisfactory state of affairs—a supernova needs to be launched most of the time to be consistent with observed rates and statistics.

What has emerged recently in the modern era of core-collapse supernova theory is that the structure of the progenitor star, the turbulence and symmetry-breaking in the core after the bounce, and the details of the neutrino–matter interaction are all key and determinative of the outcome of the collapse. Spherical simulations seldom lead to explosion. Multi-dimensional turbulent convection in the core necessitates complicated multi-dimensional radiation (neutrino)/hydrodynamic simulation codes, and these are expensive and resource-intensive. It is this complexity and the chaos in the core dynamics after implosion that have retarded progress on this multi-physics, multi-dimensional astrophysical problem, until now. In the first era of core-collapse supernova simulations, the state of the art was good spherical codes that handled the radiation acceptably. These models rarely, if ever, exploded. Multi-dimensional codes were not yet useful. Then, two-dimensional (2D; axisymmetric) codes arrived, captured some aspects of the overturning convection about which one-dimensional (1D) models are mute, but were slow—only a few runs could be accomplished per year. This era was followed by the advent of some three-dimensional (3D) capability, and at the same time many 2D runs could be performed to map out some of parameter space and gain intuition concerning the essential physics and behaviour. We are now in the era of multiple 3D simulations per year, wherein we can explore core dynamics and explosion in three dimensions, without the fear that a mistake in a single expensive run that could take a year on a supercomputer would set us back. This progress has been enabled by the parallel expansion of computer power over the decades. It is the pivotal role of multi-dimensional turbulence and the breaking of spherical symmetry in the mechanism of explosion itself, coupled with the driving role of neutrino heating, that necessitated the decades-long numerical and scientific quest for the mechanism of core-collapse supernovae. What nature does effortlessly in a trice has taken humans longer to unravel.

However, there are recent strong indications that the dominant explosion mechanism and rough systematics of the outcomes with a progenitor star are indeed yielding to ongoing multi-pronged international theoretical efforts. Moreover, code comparisons are starting to show general concordance[2]. Many recent multi-dimensional simulations employing sophisticated physics and algorithms are exploding naturally and without artifice. These include those reported by our group[3–10], those using the state-of-the-art code Fornax[11] and other studies[12–21]. Neutrino heating in the so-called gain region behind a stalled shock, aided by the effects of neutrino-driven turbulence and spherical symmetry breaking, together seem, in broad outline, to be the agents of explosion for the major channel of core-collapse supernovae. Other subdominant channels might be thermonuclear (relevant to the question of what the terminal cores of about $8M_{\odot}$–$9M_{\odot}$ stars actually do)[22–25] or magnetically driven (so-called 'hypernovae', with a frequency of about 1%[26,27]; long soft-γ-ray bursts, with frequency <0.1%). Indeed, for the neutrino mechanism numerous interesting complications

[1]Department of Astrophysical Sciences, Princeton University, Princeton, NJ, USA. [2]Department of Astronomy, University of California, Berkeley, CA, USA. ✉e-mail: burrows@astro.princeton.edu

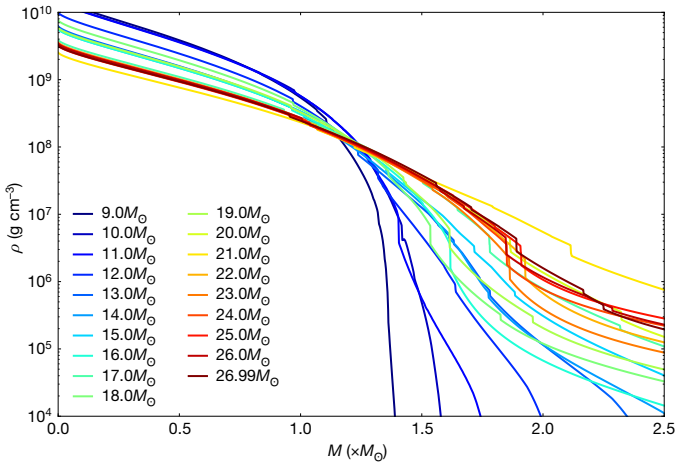

Fig. 1 | Progenitor mass density profiles. Profiles of mass density ρ versus interior mass M for the cores of the progenitor massive stars used as initial conditions for the supernova simulations highlighted in this paper. The associated spherical stellar evolution models were calculated by Sukhbold et al.[61,70] up to the point of core collapse, at which point they were mapped into our supernova code FORNAX[11].

concerning nuclear and neutrino physics, the progenitor structures, and numerical challenges remain to be resolved.

How do core-collapse supernovae explode?

It is generally agreed that the stall of the roughly spherical bounce shock wave sets up a quasi-hydrostatic structure in its interior that accretes the matter falling through the shock from the outer core that is still imploding[28–31]. The rate of accretion ($\dot{M}$) through the stalled shock and onto the inner core is an important evolving quantity that depends essentially on the density structure of the progenitor's core just before the Chandrasekhar instability (see Fig. 1) and determines much of what follows. The core is so dense and the neutrino particle energies are so high (tens to hundreds of megaelectronvolts), that the structure interior to about 10^{11} g cm^{-3} is opaque to neutrinos of all species; the structure is a 'neutrino star', and the 'neutrinosphere' radius is initially about 30–60 km and depends on the neutrino species and particle energy. The bounce shock initially forms in the deeper neutrino-opaque region, but as it emerges quickly (within milliseconds) to larger radii and lower densities, a burst of electron neutrinos (ν_e) is generated. It is this burst that saps energy from the shock and leads to its stalling into accretion. A secondary cause of the stalling is the shock dissociation of the infalling nuclei into nucleons. This effect lowers the effective adiabatic index γ of the gas, which connects the internal thermal energy with the pressure by diverting energy into nuclear breakup, thereby channelling less efficiently the gravitational energy that is otherwise available to provide pressure support for the shock. The stalled-shock radius initially ranges around 100–200 km. Just interior to the shock is the semi-(neutrino-) transparent 'gain region', where the 'optical' depth to neutrinos is about 0.1. This region surrounds the neutrinospheres through which most of the ongoing prodigious neutrino emissions emerge, and these bound the inner dense core containing most of the proto-neutron star (PNS) mass. This quasi-stable PNS bounded by the stalled shock fattens by accretion and shrinks by neutrino loss. The neutrino emissions are powered by thermal diffusion from the interior and the gravitational power of accretion. The goal of theory is to determine how the shock is reenergized and launched into explosion, leaving behind the bound neutron star. The explosion occurs at the mantle of the PNS, approximately exterior to the neutrinospheres, and the bound inner material must be left behind.

If there were no ongoing accretion, then neutrino heating in the gain region behind the shock wave would be more than sufficient to power an exploding shock. There would be no tamping accretion ram pressure, and neutrino heating by electron neutrino (ν_e) and electron antineutrino ($\bar{\nu}_e$) absorption on free neutrons and protons in the gain region would easily power a dynamical outflow. This is similar to a thermal wind. However, the accretion ram and neutrino heating compete to determine instability to explosion, with the added complication that accretion also powers a changing fraction of the driving neutrino luminosities. The explosion is akin to a bifurcation between quasi-stationary accretion and explosion solutions, with control parameters related to the accretion rate and the neutrino luminosities, but a simple analytic explosion condition in the context of realistic simulations has not yet been achieved. Hence, detailed simulations are required.

What has emerged is that only those progenitor models with very steep outer density profiles that translate into rapidly decreasing post-bounce accretion rates can explode in spherical symmetry (1D) via the neutrino mechanism. Among the representative progenitor models shown in Fig. 1, only the $9M_\odot$ star comes close to fitting that description. However, not even that star explodes in our 1D simulations. Multi-dimensional simulations seem to be required. Classically, the $8.8M_\odot$ model of Nomoto[32] explodes spherically, as do a few others with similar very steep outer density profiles[3,33]. The current explosion paradigm for most massive stars is gravitational-energy sourced, neutrino-driven and turbulence-aided, and we summarize some of what we have learned concerning the roles of various specific physical effects.

Efficiency. Given that a hot and lepton-rich PNS radiates about 3×10^{53} erg in neutrinos as it transitions into a tightly bound, cold neutron star, and supernova explosion energies are 'typically' one bethe (10^{51} erg), it is often stated that the neutrino mechanism of core-collapse explosion is one of less than 1% tolerances. This is not true. During the timescales of hundreds of milliseconds to a few seconds after the bounce, over which the neutrino heating mechanism operates, the efficiency of energy deposition in the gain region—the fraction of the emitted energy absorbed there—is about 4–10%, far higher. Most of the binding energy of the neutron star is radiated over a period of a minute[34], after the phase during which we think the explosion energy is fully determined.

Turbulent convection. Turbulence is fundamentally a multi-dimensional phenomenon and cannot be manifest in spherical (1D) symmetry (and, therefore, in 1D simulations). The turbulence in the gain region interior to the stalled shock is driven predominantly by the neutrino heating itself, which produces a negative entropy gradient that is unstable to overturn. This is similar to boiling water on a stove, via absorptive heating from below[34]. The top panel of Fig. 2 depicts the inner turbulent convective region early after the bounce and before the explosion, showing accreted matter tracers swirling randomly about the PNS core. A larger neutrino heating rate will increase both the vigour of the turbulence and the entropy of this mantle material. The matter that accretes through the shock on its way inwards to the PNS during the pre-explosion phase contains perturbations[17,35–38] that arise during pre-collapse stellar evolution, which will seed the convective instability. The larger and more prevalent these seeds are, the quicker the turbulence grows to saturation and in vigour. One feature of turbulence is turbulent pressure. The addition of this stress to the gas pressure helps to push the shock to a larger stalled-shock radius. This places matter in more shallow reaches of the gravitational potential well, out of which it must climb, and helps to overcome the subsequently smaller ram pressure due to infalling matter from the outer core still raining in. The turbulence also forces the accreted matter to execute non-radial trajectories as it settles, increasing the time during which it can absorb neutrino energy before settling on the PNS and, hence, the average entropy that can be achieved in the gain region[39]. Therefore, through the combined agency of both neutrino heating and

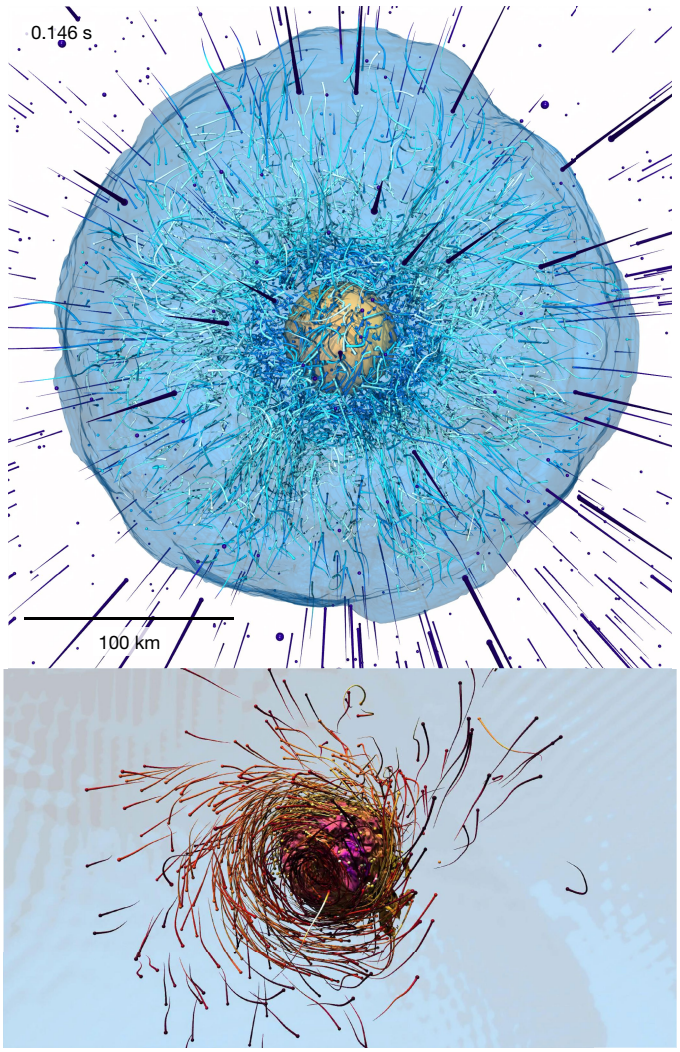

Fig. 2 | Turbulence in the belly of the beast. Top, inner matter trajectories as the explosion is about to launch. Shown are the interiors of an explosion only about 150 ms after core bounce (vertical physical scale, about 350 km). At this time, the shock wave is at about 150 km, just before explosion. The inner ball is the newly birthed PNS (rendered as an isodensity surface at 10^{11} g cm^{-3}; coloured by Y_e; yellow is low electron fraction), surrounded by swirling, turbulent matter, most of which will settle onto the PNS. The trajectories depict the recent 5 ms in the positions of individual accreted matter elements, and they are coloured by local entropy (dark blue is low entropy and light green is high entropy). The turbulence of this inner region is evident. Bottom, generic swirling motions just exterior to the PNS, a few hundred milliseconds after explosion. The physical scale top to bottom is about 200 km. Upon accretion into this inner region, the matter blobs can stream to the one or the other side of the core before finally settling onto it. This stochastic, almost random, accretion of angular momentum can sum over time to leave a net angular momentum and spin, despite the fact that the original progenitor model was non-rotating[87,100–102].

neutrino-driven turbulence, the quasi-stationary structure that is the PNS plus the mantle plus the stalled-shock wave is more likely to reach a critical condition wherein the steady infalling solution bifurcates into an explosive one. The huge binding energy accumulated in the PNS does not need to be overcome—only its mantle (and with it, the rest of the star) needs to be ejected.

Moreover, the turbulent hydrodynamic stress is anisotropic, with its largest component along the radial direction[39]. Turbulent magnetic stress might also be a factor[40]. Importantly, turbulence is more effective at using energy to generate stress/pressure than a gas of nucleons, electrons and photons. As much as about 30–40% of the stress behind the stalled shock can be in turbulent stress when the turbulence is fully developed. Hence, partially channelling gravitational energy of infall into turbulence instead of into thermal energy helps to support and drive the shock more efficiently[8].

Neutrino–matter Interactions. The predominant processes by which energy is transferred from the radiated neutrinos to the matter behind the shock in the gain region are electron neutrino absorption on neutrons via $\nu_e + n \rightarrow e^- + p$ (n, neutron; e^-, electron; p, proton), electron antineutrino absorption on protons via $\bar{\nu}_e + p \rightarrow e^+ + n$($e^+$, positron), and inelastic scattering of neutrinos of all species from both electrons and nucleons. The two super-allowed charged-current absorption reactions dominate and provide a power approximately equal to the product of the neutrino luminosity and the neutrino optical depth in the gain region; the latter can be about 10%. Therefore, the higher the luminosity and/or absorption optical depth is, the greater the neutrino power deposition is, which can reach levels of many bethes per second. Upon explosion, most of this power goes into work against gravity, and only a fraction of the deposited energy is left as the asymptotic blast kinetic energy. This is very qualitatively similar to a thermally driven wind, for which the energy at infinity scales with the binding energy of the ejecta. Therefore, the stellar binding energy of the ejected mantle might approximately set the scale of the supernova explosion energy. We discuss aspects of this paradigm in section 'Supernova energies'.

At higher mass densities (ρ), above 10^{11}–10^{12} g cm^{-3}, nucleon–nucleon interactions introduce correlations in density and spin. Such non-Poissonian correlations modify the neutrino–matter scattering and absorption rates (generally suppressing them), thus affecting the emergent neutrino luminosities[41–46]. This is relevant to the instantaneous power deposition in the gain region, and hence the neutrino-driving mechanism itself. These many-body effects increase with density, and some of the associated correction factors have been estimated[47,48] to be of the order of 10–20% at 10^{12} g cm^{-3}, near and just interior to the neutrinospheres. However, such corrections depend on a detailed and self-consistent treatment of the opacities along with the nuclear equation of state, and this goal has yet to be achieved. Nevertheless, the use of scattering suppression factors[4,48] has shown that these effects can facilitate explosion by decreasing the opacities, thereby increasing the neutrino loss rates. This leads to a more rapid shrinking of the PNS, which, owing to consequent compression, heats the neutrinosphere regions. This increases the mean energy of the emitted neutrinos. Given that the rates of neutrino absorption via the charged-current reactions quoted above increase approximately as the square of the neutrino energy and the luminosities themselves are elevated, the neutrino power deposition in the gain region is augmented, thereby facilitating explosion. The effect is not large, but when an explosion is marginal, it can be determinative.

During the early collapse phase, increasing densities lead to increasing electron Fermi energies and higher electron capture rates on both free protons and nuclei. Electron capture decreases the electron fraction (Y_e; the ratio of the electron density to the proton plus neutron density) of the infalling gas, and this decreases the electron pressure. A decrease in the electron pressure slightly accelerates the infall and the mass-accretion rate ($\dot{M}$) versus time. As already stated, $\dot{M}$ after inner-core bounce is a key parameter that determines, among other things, the accretion ram pressure external to the shock and the accretion component of the neutrino luminosities. Therefore, the rate of capture on infall can affect the timing, and perhaps the viability, of the explosion. The effect is not large, but when things are marginal, altering the evolution of $\dot{M}$ can be important. However, the capture rate on the mix of nuclei in the imploding core is not known to better than a factor of five[49–51]. Hence, clarifying this important issue remains of interest to modellers.

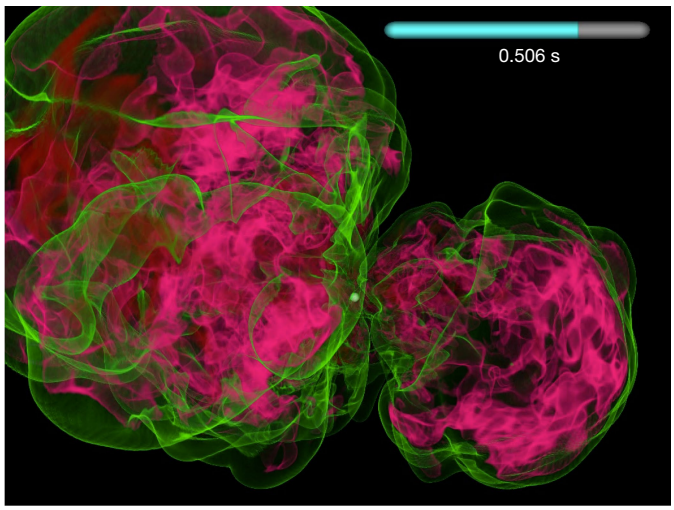

Fig. 3 | Early 3D explosion of the core of a 16$M_\odot$ star using FORNAX. Still near 500 ms after core bounce at nuclear densities. The red colour shows a volume rendering of the high entropy of the ejecta in the neutrino-heated bubbles that constitute the bulk of the volume of the exploding material. The green surface is an isoentropy surface near the leading edge of the blast, the supernova shock wave. Note the asymmetric, although roughly dipolar, character of the explosion and the pinched 'wasp-waist' structure of the flow between the lobes. The dot at the centre is the newly born neutron star. In this model, as in many others, there is clearly simultaneous accretion at the waist and ejection in the wide-angle lobes. Simultaneous accretion in one sector during concommitant explosion elsewhere maintains the driving neutrino luminosity and is a signature of the useful breaking of spherical symmetry that is possible in multi-dimensional flow. This contrasts sharply with the artificially enforced situation in 1D/spherical simulations. Simulation performed by the Princeton supernova group[6].

Finally, the energy transfer to matter via inelastic scattering off electrons and nucleons provides a subdominant component of the driving heating power behind the shock wave. The effect may be only 10–15%, but, again, when the core teeters on the edge of explosion, such effects matter. Neutrino scattering off electrons (akin to Compton scattering, but for neutrinos) results in a large energy transfer but has a small rate. Energy transfer to the heavier nucleons is small, but the scattering rate is large. The net effect results in comparable matter-heating rates for both effects, with a slight advantage to neutrino–nucleon scattering[4]. However, calculating such spectral energy redistribution is numerically difficult and represents one of the major computational challenges in the field[44,52,53].

Explosion. The stalled-shock radius can be decomposed into spherical harmonics in solid angle. The onset of the explosion of a stalled accretion shock is a monopolar instability in the quasi-spherical shock. However, approximately when the monopole becomes unstable, the dipole often seems to do so as well[6,54]. Therefore, the explosion picks an axis, seemingly at random for a non-rotating progenitor, and the blast has a dipolar structure with a degree of asymmetry that seems to be low for quickly exploding models and larger for those with more delayed explosion. Figure 3 depicts an example blast structure manifesting such a dipole[6]. Generally, but not always, lower-mass progenitors (such as a 9$M_\odot$ progenitor[7,9]) explode earlier and before turbulence is vigorous, and more massive progenitors seem to explode later and after turbulence has achieved some vigour. Hence, the latter usually explode more asymmetrically, with a larger dipolar component[55]. The chaos of the turbulence makes the outcome stochastic, so that the direction of explosion is not easily predicted. Importantly, the chaos of the turbulent flow will result in distribution functions of explosion times, directions, explosion energies, explosion morphologies, residual neutron-star masses, ^{56}Ni yields, general nucleosynthesis and kick velocities, even for the same star. It is not even known whether those functions are broad or narrow for a given star.

In addition, exploding more along an axis, as depicted in Fig. 3, allows the flow external to the shock to wrap around the prevailing axis and accrete along a pinched waist in an equatorial structure. This breaking of symmetry, which is impossible in spherical symmetry, allows simultaneous accretion and explosion. Whereas a 1D explosion by its nature turns accretion off in all directions, and thereby throttles back the accretion component of the driving neutrino luminosity, in multi-dimensional models the accretion component of the luminosity can be maintained. Hence, the breaking of spherical symmetry supports the driving luminosity and facilitates explosion just as it is getting started. This symmetry breaking is an important aspect of viable explosion models and is impossible in spherical models. Nature unchained to manifest overturning instability leading to turbulence employs this freedom to facilitate explosions that might be thwarted in one dimension. Both the turbulent stress and the option of simultaneous accretion in one direction while exploding in another one are important features of the core-collapse supernova explosion mechanism.

Convection in the progenitor star upon collapse will create perturbations in velocity, density and entropy that seed overturn and turbulence in the post-shock matter exterior to the inner PNS and the neutrinospheres. The magnitude of these perturbations generally increases with progenitor mass, but their true character is only now being explored in detail. Recently, a number of groups have embarked upon 3D stellar evolution studies during the terminal stages of massive stars[17,22,24,56–58]. The potential role of aspherical perturbations in the progenitor models in inaugurating and maintaining turbulent convection behind the stalled-shock wave is an active area of research[4,5,17,37,58], and these studies might soon reveal the true nature of accreted asphericities and their spatial distribution. It might also be that low-order modes in the progenitors would naturally result in angular asymmetries in mass accretion through the shock and provide a path of least resistance that would (however randomly) set the explosion dipole and direction, whatever its magnitude. Such low accretion-rate paths might actually facilitate explosion in circumstances in which it would otherwise be problematic.

Another convective phenomenon that can help to achieve the critical condition for explosion is PNS convection. This is not the neutrino-heating-driven convection in and near the gain region just behind the stalled shock, but overturn driven by lepton loss from beneath the neutrinospheres. As electron neutrinos are liberated from the inner PNS mantle around a radius of about 20 km, the resulting negative Y_e gradient is convectively unstable. This is akin to instabilities in stars due to composition gradients. All PNSs show this instability, which lasts for the entire duration of PNS evolution and probably continues long (many seconds to one minute) after the explosion is launched (if it is). PNS convection[10,59,60] accelerates energy loss (particularly via ν_μ, ν_τ, $\bar{\nu}_\mu$ and $\bar{\nu}_\tau$) and lepton loss in the PNS, thereby accelerating core shrinkage. In a manner similar to the many-body effect, such core shrinkage leads to higher neutrinosphere temperatures and a stronger absorptive coupling to the outer gain region.

We end this section by emphasizing that the most important determinant of explosion, all else being equal, is the mass density structure of the unstable Chandrasekhar core. The density profile translates directly into the mass-accretion rate after bounce, and this determines both the accretion tamp and the accretion component of the driving neutrino luminosity. Figure 1 provides an example set[61] of density profiles $\rho(r)$ from 9$M_\odot$ to 27$M_\odot$. This set spans most (but not all) massive stars that give birth to core-collapse supernovae. There are a few trends in $\rho(r)$ that are worth noting. First, the lowest-mass massive stars generally have slightly higher central densities and steeper outer profiles and the higher-mass massive stars have lower central densities and much shallower outer density profiles. However, the trend in the slope of the outer density profiles is not strictly monotonic with progenitor

mass, with some 'chaos' in the structures. Ambiguities in the handling of convection, overshoot, doubly diffusive instabilities and nuclear rates have led to variations from modeller to modeller in progenitor stellar models up to collapse, which have yet to converge. Furthermore, the effects of fully 3D stellar evolution and rotation have not yet been fully assessed. Therefore, the summary behaviour depicted in Fig. 1 is provisional.

Given these caveats, important general insights are emerging. The first is that the silicon/oxygen shell interface in progenitors (seen for many models in Fig. 1) constitutes an important density jump, which—if large enough—can kickstart a model into explosion. In many of our models, the shock is 'revived' upon encountering this interface[9,62]. The associated abrupt drop in accretion rate and inhibiting ram pressure at the shock upon the accretion of this interface is not immediately followed by a corresponding drop in the driving accretion luminosity. This is due to the time delay between accretion to the shock at 100–200 km and accretion to the inner core, where the gravitational energy is converted into useful accretion luminosity. This time delay pushes the structure closer to the critical point for explosion. However, sometimes the density jump is not sufficiently large, and its magnitude in theoretical stellar models has not been determined definitively.

Second, the very steep density profiles seen for the lower-mass massive stars lead to earlier explosions. However, the associated steeply decreasing rates of accretion also result in less mass in the gain region and a lower optical depth to the emerging neutrino fluxes. The lower absorption depths in the mantle multiplied by the lower neutrino luminosities lead to lower driving powers in the exploding mantle. This results in lower explosion energies generically under the neutrino heating paradigm for those stars with steep outer density profiles. Conversely, those stars with shallow density profiles, more often the more massive core-collapse supernova progenitors, generally explode later. However, their shallow mass profiles result in more mass in the gain region with a greater optical depth. The larger depths multiplied by the larger accretion luminosities lead to greater driving neutrino power deposition. The net effect is often higher asymptotic supernova explosion energies. Hence, with exceptions, state-of-the-art models suggest that the explosion energy is an increasing function of progenitor mass and the shallowness of the outer density profile of the initial core. In addition, 'explodability' does not seem to be a function of 'compactness'[4,62,63] (a measure of the ratio of the progenitor interior mass to its radius), with both high- and low-compactness models exploding. It had been suggested that only low-compactness structures exploded. Not only does this not seem to be true, but it appears that only the higher-compactness models can result in explosion energies near the canonical 1 bethe. It may be, however, that very-high-compactness structures have outer-mantle binding energies for which the neutrino mechanism cannot provide sufficient driving power. These objects may lead to either weak explosions or fizzles, with many of these leading to black holes (and not neutron stars). In fact, the gravitational binding energy of the mantle of the Chandrasekhar core may set the scale of the explosion energy and, if too high, might thwart explosion altogether. This topic deserves much more attention.

Supernova energies

2D (axisymmetric) and 3D simulations do not behave in the same way. The axial constraint and artificial turbulent cascade of the former compromise the interpretation of the results. However, 2D simulations do allow the breaking of important symmetries and overturning motions, and are less computationally expensive to perform. Importantly, owing to their much lower cost, 2D numerical runs can easily be carried out to many seconds after the bounce—something that we, and others, have found that many stars require to asymptote to their final blast kinetic energies in the context of the neutrino mechanism[64]. Therefore, to get a bird's eye view of the systematic behaviour of the explosion as a function of progenitor mass, we have conducted a suite of longer-term

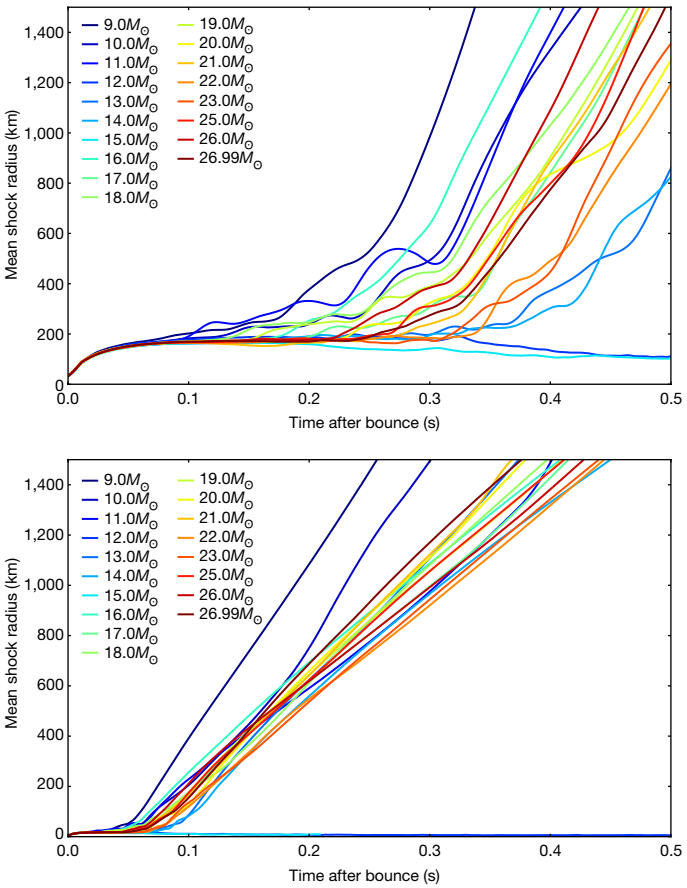

Fig. 4 | Mean shock radii of 2D models. Depicted are the angle-averaged shock radii calculated with the 2D model suite versus time after the bounce. Most of the models explode, whereas the $12M_\odot$ and $15M_\odot$ progenitor structures do not. The top panel shows the behaviour during the first 0.5 s after the bounce and in the inner 1,500 km, with models exploding (when they do) between 0.15 s and 0.4 s. The bottom panel shows the shock motion on a larger physical scale (15,000 km) and to later times. Many of the models were carried to about 4.5 s after the bounce. The mean shock speeds become stable, with values of 10,000–15,000 km s^{-1} for most of the simulation. The simulations were conducted on grids of 30,000–100,000 km, with smaller values for the smaller-mass progenitors. See the footnote of Table 1 for specifics.

2D simulations using the stellar models of Sukhbold et al.[61] as starting points. For this collection, we have usually found that when a 2D model explodes, its more realistic 3D counterpart does as well, and when it does not, neither does the 3D simulation. In our experience, this is usually—but not always—the case, although there is some disagreement on this in the literature[15,18,54,65–69]. In our recent set of models, it is only the $12M_\odot$ and $15M_\odot$ models that do not explode. The 2D models generally seem to explode slightly earlier than the 3D models. For instance, the $20M_\odot$ and $25M_\odot$ stars explode about 100 ms and 50 ms later in 3D models, respectively. Also, on average models with more massive progenitors explode later. Nevertheless, the shock is (re)launched, if it is, between about 150 ms and around 400 ms after the bounce for all these 2D exploding models. This timescale depends on the simulation details (such as microphysics, resolution and algorithms), as well as the character of the seed perturbations. For these simulations, we did not impose extra perturbations, and left the inauguration of the initial overturning instabilities to numerical noise.

Figure 4 portrays the development of the mean shock radius for all the models used in this study. The top panel shows the launch phase, and the bottom panel provides a later, larger-scale glimpse. The mean shock speeds settle between 10,000 km s^{-1} and 15,000 km s^{-1}. Table 1

Table 1 | Explosion energies and neutron-star masses

Model (×$M_\odot$)	Explosion energy (bethes)	Run time (s)	Baryonic mass (×$M_\odot$)	Gravitational mass (×$M_\odot$)
9	0.09	2.34	1.35	1.23
10	0.15	3.36	1.49	1.35
11	0.15	3.52	1.51	1.37
12	−0.03	2.75	1.82	1.62
13	0.78	4.60	1.89	1.68
14	0.28	4.51	1.81	1.62
15	−0.17	1.04	1.93	1.71
16	0.36	4.45	1.75	1.56
17	1.86	4.66	2.05	1.81
18	1.24	4.58	1.80	1.60
19	0.63	4.45	1.87	1.66
20	1.22	4.56	2.10	1.85
21	1.74	3.76	2.27	1.97
22	0.95	4.74	2.06	1.81
23	0.73	4.55	2.04	1.80
25	1.39	3.11	2.11	1.85
26	2.3	4.60	2.15	1.88
26.99	1.17	4.60	2.12	1.86

The $9M_\odot$, $10M_\odot$ and $11M_\odot$ progenitor data are from the Sukhbold et al. (2016)[70] suite and were evolved on spherical grids with radial extents of 30,000, 50,000 and 80,000 km, respectively. Progenitors from $12M_\odot$ to $26.99M_\odot$ were inherited from the Sukhbold et al. (2018)[61] suite. The $12M_\odot$, $13M_\odot$ and $14M_\odot$ progenitors were evolved on a spherical grid spanning 80,000 km in radius. All other progenitors were evolved on spherical grids spanning 100,000 km in radius. All models were evolved in 2D axisymmetry with 1,024 radial cells and 128 (θ) angular cells. Thus, there are some small differences in resolution for the lower-mass progenitors, where the progenitor grid is truncated at smaller radii so that the temperature remains within our equation-of-state table. All models except the $12M_\odot$ and $15M_\odot$ progenitor ones explode. The run time quoted is the time after bounce at nuclear densities.

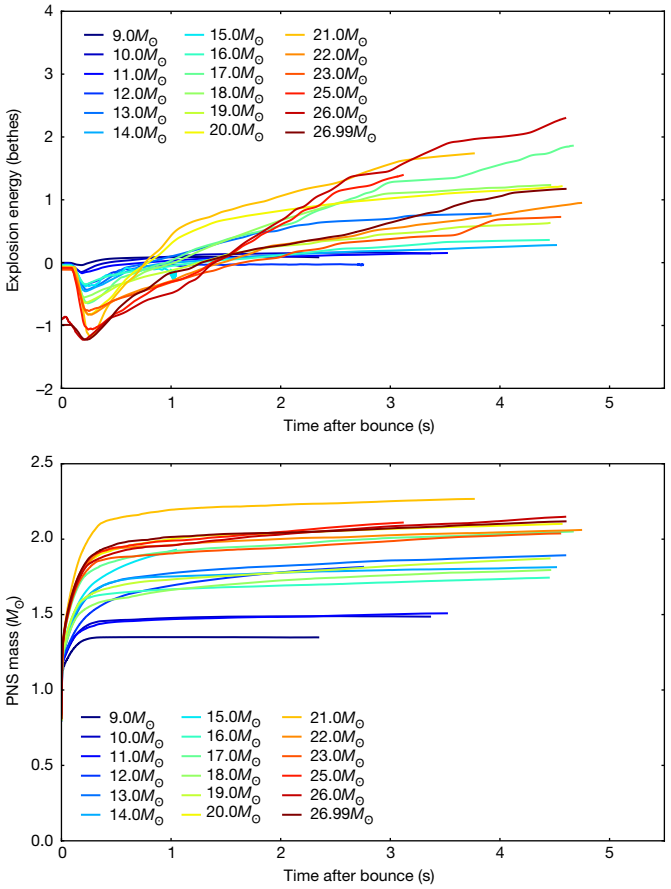

Fig. 5 | Explosion energy and residual neutron star baryon mass. Top, evolution of the total explosion energy with time. As the figure indicates, many models start as bound (negative energies), even though their shocks have been launched. It can take more than one second for some to achieve positive energies—the true signature of an explosion. Moreover, it can take about 4–5 s for the supernova energy to asymptote, and some take longer than that; all the more massive exploding models take this longer time, and they generally achieve the highest supernova energies. The lower-mass massive progenitors asymptote earliest at generally—although not universally—lower supernova energies. In addition, although a model might explode late, it can still achieve a higher explosion energy than those that explode early. Hence, the time of explosion is not indicative of its eventual vigour. We note that the $12M_\odot$ and $15M_\odot$ stars in this investigation do not explode. Bottom, theoretical baryon mass of the residual neutron star versus time after bounce for the 2D models used in this study. The evolution of the residual neutron-star mass is generally quick, with the final mass determined to within about 5% generally (though not universally) within about 1 s of the bounce. The range of residual masses ranges from about $1.3M_\odot$ to $2.2M_\odot$ for this model set. This is equivalent to a range of neutron-star gravitational masses between about $1.2M_\odot$ and about $2.0M_\odot$, roughly what is seen empirically. Generally, the lower-mass progenitors give birth to lower-mass neutron stars, although this is not rigorously monotonic. We note that the $12M_\odot$ and $15M_\odot$ models that do not explode are still gradually increasing their residual masses by the end of those simulations (see Table 1).

lists the explosion energy, baryonic and gravitational masses, and post-bounce run time. The energies have asymptoted to within a few tens of per cent of their final supernova energies for all models and range from 0.09 to 2.3 bethes. The $24M_\odot$ model is being further scrutinized and is not included here. The higher energies are statistically, but not monotonically, associated with more massive progenitors. The growth of the blast energy is depicted in the top panel of Fig. 5. Those models that asymptote early do so at lower energies. Those models that eventually achieve higher explosion energies not only do so later, but experience deeper negative energies for a longer time before emerging into positive territory. As described in section 'How do core-collapse supernovae explode?', this is what is expected for models with massive (shallow) density mantles, if they explode, and these are generally—although not exclusively—for the most massive progenitors (>$16M_\odot$).

The energies shown in Table 1 and Fig. 5 include the gravitational, thermal and kinetic energies, as well as the nuclear reassociation energies, of the ejecta. They also include the outer-mantle binding energies of the as-yet-unshocked material. In this way, all the components of the blast energy are accounted for, except the thermonuclear term. The latter could be as much as about 10% of the total, and will slightly increase our numbers. However, $0.1M_\odot$ of oxygen provides only about 0.1 bethe, so it is only for the most explosive progenitors with sizable oxygen and carbon shells for which these mostly gravitation-powered supernovae can have an interesting thermonuclear component; this might still be only about 10%. One would expect that the ^{56}Ni yields would be higher for the more densely mantled stars, so that the thermonuclear energy contribution and ^{56}Ni yield would be correlated with one another and with the progenitor mass[70,71]. Curiously, if the speculations[22] concerning the thermonuclear character of the lowest-mass progenitors bear out, this correlation might be preserved, but for the other end of the massive-star mass distribution ('mass function'). We note that the mass function is weighted towards the lower masses.

Figure 6 superposes the theoretical explosion energies of Table 1 onto a plot of the observationally inferred type IIp (plateau) supernova energies versus inferred ejecta masses. For our theory numbers, we shift the initial progenitor mass by $1.6M_\odot$ to account for an average residual neutron star. In so doing, we do not account for the pre-explosion mass loss of the star, which could be substantial. However, the general trend of the inferred energy with a measure of stellar mass is reproduced by

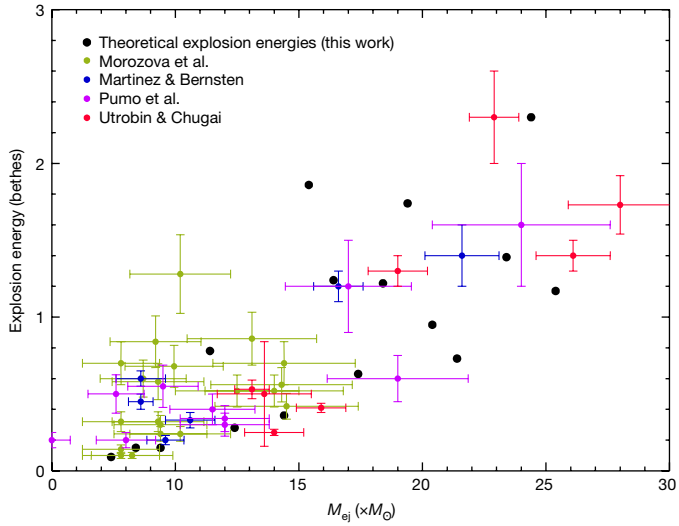

Fig. 6 | Comparison of theoretical and empirical explosion energy versus ejecta mass. Plotted are the empirically inferred explosion energies versus the inferred ejecta masses, with error bars, for a collection of observed type IIp (plateau) supernovae. Our theoretical numbers, taken from Table 1, are superposed as black dots. It must be recalled that these are 2D models, and that there are quantitative differences between 2D and 3D simulations. We assume for convenience that the theoretical ejecta masses are the progenitor masses, minus the baryon mass of a putative residual neutron star of $1.6M_\odot$. This ignores any mass loss before explosion, which is an assumption that is incorrect by about $1M_\odot$–$3M_\odot$. Nevertheless, the rough correspondence between theory and measurement is encouraging. We note that the error bars on the measurement points are not firm and do not include any systematic errors in the light-curve modelling procedures. In any case, the general average trend from low to high explosion energy from lower to higher massive-star progenitor mass reflected in the observations is reproduced well by the theory, both quantitatively and qualitatively. In addition, at a given mass there is an inferred measured spread in supernova energies. This may represent a real variation in explosion energy at a given progenitor mass due in part to the natural chaos in turbulent flow. Indeed, it is theoretically expected that nature would map a given star's properties to distribution functions in the outcomes and products of its supernova death. The empirical estimates were taken from Morozova et al.[103], Martinez & Bersten[104], Pumo et al.[105,106] and Utrobin & Chugai[107–110].

the theoretical calculations (black dots in Fig. 6). There is scatter in both the theory and observations, the latter due to systematic uncertainties in the models employed and observational limitations, and the former due to numerical and astrophysical uncertainties. However, natural chaos in the dynamics would naturally lead to a spread in energies (section 'Core-collapse supernova explosions'), to a degree as yet unknown, even for the same initial stellar structure. We note that there seems to be a larger observational spread in the inferred energies at lower masses. This could reflect natural chaos in the turbulent neutrino mechanism, measurement uncertainties, the effects of unknown rotation or the possibility that the lowest-mass progenitors explode thermonuclearly just after the onset of a collapse that does not achieve nuclear densities. However, it is too soon to draw any definitive conclusions on this score. Be that as it may, the observed roughly monotonically increasing trend of explosion energy with mass and the ability of the neutrino mechanism to reproduce the observed range of explosion energies are both encouraging.

Finally, the infalling accretion matter plumes that hit the PNS core generate sound waves that are launched outwards. Much of the energy of these sound waves is absorbed behind the shock wave and can modestly contribute to the explosion energy. Such a component is automatically included in our bookkeeping. Although it is difficult to estimate separately, we do not envision that acoustic power can contribute more than about 5–10% to the total.

Residual neutron-star masses

The bottom panel of Fig. 5 depicts the evolution of the residual baryon mass of the PNS core for the suite of 2D models investigated here. Such masses cease accumulating early because the mass-accretion rates drop quickly after the explosion commences. The final baryon masses at the last timesteps are given in Table 1, as are the corresponding gravitational masses. The latter include the gravitational binding energy (negative) of the core. These masses range from a low near $1.2M_\odot$ to a high near $2.0M_\odot$, spanning the observed range[72]. The neutron-star masses that we find are closely, but not perfectly, monotonic with progenitor mass and the shallowness of the Chandrasekhar mantle, except for those models that do not explode. Presumably, these models will eventually collapse to black holes, but on timescales longer than we have simulated.

Ejecta compositions

The issue of the ejecta elemental composition is fundamental to supernova theory. The shallowness of the outer-mantle density profile and the associated mass of the inner ejecta are roughly correlated with the yields of oxygen and intermediate-mass (for example, Ar, Si, Ca) elements. As suggested in section 'Supernova energies', such a structure is also likely to explode (if via the neutrino mechanism) with higher energies. Therefore, more of these inner ejecta will be able to achieve the higher temperatures that can transform oxygen and silicon into iron-peak species as well. This includes ^{56}Ni. Therefore, one expects that in the context of the neutrino mechanism of explosion, ^{56}Ni yields are roughly increasing functions of progenitor mass, with the exceptions to strict monotonicity alluded to previously. Specifically, if a $9M_\odot$ star explodes by the neutrino mechanism, it cannot have much ^{56}Ni in its ejecta, and if a ~$16M_\odot$–$25M_\odot$ star explodes by the same mechanism, the ^{56}Ni yield should be greater.

All the inner ejecta from the region interior to the stalled-shock wave, before and just after explosion, are very neutron-rich ($Y_e \approx 0.1$–0.2). As they expand outwards, absorption by ν_e and $\bar{\nu}_e$ on balance tends to push the ejecta Y_e upwards. If the expansion is fast, then some of the ejecta will be slightly neutron-rich below $Y_e = 0.5$. However, if the expansion is slow, there is plenty of time for some of the debris to become proton-rich ($Y_e > 0.5$). However, generally $Y_e = 0.5$ seems to predominate in the bulk. Therefore, those models that explode early and fast should provide some neutron-rich ejecta, although most of their ejecta could still be proton-rich, while those models that explode later and more slowly (generally, the more massive progenitors) will be the most proton-rich. This is what we[9] see in cases with electron fractions from about 0.5 to as high as around 0.58–0.6. This might make such supernovae sites for the rp-process (rapid proton capture) and for light proton-capture nuclei (p-nuclei) (for example, ^{74}Se, ^{78}Kr and ^{84}Sr)[73–75]. However, these numbers should be viewed as preliminary, because they depend on detailed neutrino transport calculations and the complicated trajectory histories of the ejecta parcels. We note that observations of ^{57}Ni in SN1987A, which is inferred to be a ~$18M_\odot$ progenitor, require that no material with $Y_e < 0.497$ could have been ejected[76]. Also, none of the ejecta seen in modern simulations can be the site of all the r-process (the rapid neutron addition process that is responsible for the creation of half the heavy elements), although the first peak is not excluded. The timescales and electron fractions are not at all conducive.

Furthermore, as stated, inner supernova matter explodes aspherically, with bubble, botryoidal and fractured structures predominating. However, the spatial distribution of Y_e in the ejecta can have a roughly dipolar component, with one hemisphere more proton-rich than its counterpart. Figure 7 depicts a snapshot of a simulation of a $19M_\odot$ model. The bluish veil is the shock, and the fractured surface is an isoentropy surface defined by Y_e. As seen, there is an orange–purple dichotomy, which reflects the fact that the ejecta have a dipole in Y_e that persists. Even an initially uniform ejecta Y_e distribution may be

Fig. 7 | 3D explosion structure of a representative massive-star progenitor model. The associated simulation was performed with a 678 (radius) × 256 (θ, polar angle) × 512 (ϕ, azimuthal angle) grid to render slightly finer details. The snapshot was taken about 800 ms after the core bounce, about 500 ms into the explosion. The blue–grey veil is the shock wave. The coloured isosurface is of constant entropy, coloured with the electron fraction, Y_e. We note that there is a large region of purple (higher Y_e, more proton-rich) matter on one side and a largish region of orange–yellow (relatively lower Y_e, less proton-rich) matter on the other. This global Y_e asymmetry is created by persistent angular asymmetries in the emission of electron neutrinos and electron antineutrinos from the core during explosion, which, by absorption in the ejecta, create this asymmetry in the electron fraction of the ejecta. The latter translates into an asymmetry in the nucleosynthetic element angular distribution. Results derived from a simulation carried out by the Princeton supernova group[8].

unstable to the establishment of such a dipole. If near and exterior to the ν_e neutrinosphere at the 'surface' of the PNS, a perturbation in Y_e arises in a given angular patch of the inner ejecta, and that perturbation can grow owing the concommitant effect on the absorptive opacity at those angles; this in turn will either suppress or enhance the ν_e emissions to push the Y_e evolution of that matter parcel in the same direction. The progressive diminution of this absorptive Y_e shift effect with distance can freeze the Y_e perturbation. The upshot is then a crudely dipolar distribution in Y_e that tracks a crudely dipolar angular distribution in the ν_e and $\bar{\nu}_e$ luminosities and the so-called LESA (lepton emission sustained asymmetry) phenomenon[18,55,77,78]. Whether this dipolar asymmetry in Y_e in the ejecta is a generic outcome remains to be seen.

Pulsar proper motions and kicks

The neutron stars born as PNSs in the supernova cauldron are the source of the radio pulsars known to be darting throughout the Galaxy with speeds that average about 350 km s^{-1} (refs. [79,80]) and can reach about 1,500 km s^{-1} (ref. [81]). The most natural explanation for these galactic motions is recoils produced during the supernova explosion that are directly related to asymmetric matter ejection[82–88] and/or asymmetric neutrino emission. Hence, momentum conservation in the context of occasionally very aspherical ejection can easily yield the observed speeds. Moreover, it is known that neutrino emissions can have a dipolar component and that the associated net momentum can be large. Neutrinos travel at velocities extremely close to the speed of light c and constitute in sum as much as $0.15M_\odot c^2$ of mass-energy. Therefore, a mere 1% asymmetry in angle can translate into a kick of about 300 km s^{-1}. However, it is not known how the ejecta and neutrino momentum vectors sum, in particular whether they add or subtract, and what the integrated magnitude of the latter is.

Nevertheless, one can speculate about the trends as a function of progenitor star mass of the magnitude of the kicks experienced[89]. We have seen that the lowest-mass massive stars tend to explode slightly more spherically, eject less core mass and emit less energy in neutrinos. The radiated binding energies of the PNS are lower, given the lower accretion rates and lower PNS mass. Hence, we expect the kicks to be smaller for the lower-mass progenitors. Conversely, the more massive progenitors tend to explode slightly more aspherically, ejecting more core mass and emitting more mass-energy in neutrinos. Hence, we posit that they produce neutron stars with the greatest kick speeds. There is likely to be some noise in these suggestions, but on average these trends with progenitor mass (actually, progenitor structure; see Fig. 1) are compelling in the context of the neutrino mechanism of core-collapse supernova explosions. Moreover, one would predict that stellar-mass black holes born in the context of core collapse would have low kick speeds, given that they are generally expected to have much more inertia/mass than neutron stars, and the momentum in any matter ejecta that their birth may entail should be smaller. However, the neutrino kicks may be as considerable as for neutron-star birth; therefore, the momentum in any such black-hole birth kick might be comparable.

Black-hole formation

If and when the PNS mass exceeds the maximum gravitational mass of a neutron star (with suitable small thermal and compositional corrections), it will collapse to a black hole and continue to accrete. This maximum mass is $2.1M_\odot$–$2.4M_\odot$ gravitational and about $2.4M_\odot$–$2.7M_\odot$ baryonic, and depends on the modestly constrained nuclear equation of state. How much mass is subsequently accreted depends on how much of the progenitor star is ejected. If none of the star is ejected and (1) most of the progenitors of such stellar-mass black holes are the higher-mass massive stars with high envelope binding energies (see section 'How do core-collapse supernovae explode?') and (2) these have experienced substantial pre-collapse wind and/or episodic mass loss, then one would expect the canonical mass of the product black hole to be about $10M_\odot$–$20M_\odot$ (ref. [90]). This is the helium core mass of those model stars that have very high envelope binding energies exterior to the Chandrasekhar core. However, we[9] had earlier witnessed that stars with initial masses in the $13M_\odot$–$15M_\odot$ range did not explode. This result could easily be model-dependent and is not the final word on what such stars do. Nevertheless, it is possible that the black-hole outcome is peppered about the massive-star mass function[62,70,91–93]. However, the consensus is that most massive stars with initial masses lower than about $20M_\odot$ will lead to neutron stars and most stars with initial masses greater than about $30M_\odot$ should lead to black holes.

If most stellar-mass black holes birthed via collapse have masses of the order of $10M_\odot$ and neutron stars have a maximum mass slightly above about $2.0M_\odot$, then there would be a 'mass gap' between them. Such a gap is suggested by the data but has not been proven[90,94]. It may be that a shock is relaunched, but has insufficient energy to eject enough of the inner mass, and then falls back, still launching an explosion wave that unbinds the rest of the stellar envelope. Where this mass cut occurs would determine the birth mass of such a black hole. A 'fall-back' black hole is a distinct possibility[92] but may be a small subset of the massive-star mass function. It is likely that most collapses lead to neutron stars, but what the neutron-star/black-hole birth ratio is for the population of massive stars is a subject of much current research.

Finally, there are a few points of principle that need to be articulated. The first is that in the context of the collapse of a Chandrasekhar core, it is impossible to collapse directly to a black hole—there must always be a PNS intermediary. This is because the bouncing inner core is out

of sonic contact with the outer infalling core. At the bounce, the object does not know that it will eventually exceed the maximum mass. This means that even when a black hole is the final outcome, the PNS core will always have an important neutrino[95] and gravitational-wave[96] signature. A signature of the subsequent dynamical collapse to a black hole will be the abrupt cessation of both signals[97]. In addition, given that neutrino energy losses in the range of about $0.1M_{\odot}c^2$–$0.4M_{\odot}c^2$ are inevitable, the outer stellar envelope will experience a decrease in the gravitational potential that it feels. This will lead to its readjustment on dynamical timescales and probably the ejection of matter to infinity[98,99]. Hence, there should always be some sort of explosion, even when a black hole forms. Whether it is such a 'potential-shift' explosion, one with considerable fallback, or one via a disk jet after the black hole and accretion disk form, it is difficult to imagine a purely quiescent black-hole birth.

Final thoughts

As should now be clear, from the vantage of theory, a multitude of effects are of importance in determining the viability, character and strength of a core-collapse supernova explosion. The roles of the initial progenitor structure; multi-dimensional neutrino radiation transport; general relativity; instabilities, turbulence and chaos; the nuclear interaction and equation of state; neutrino–matter processes and many-body effects; resolution and numerical technique; rotation; and magnetic fields must all be assessed on the road to a resolution of this complex problem. It is this complexity that has paced progress on this multi-physics, multi-dimensional and multi-decade puzzle. However, modern theory has grappled with all these issues and inputs, with the result that state-of-the-art simulations from many groups evince explosions via the neutrino mechanism with roughly the correct general character and properties. Not all researchers agree on the details, nor do they obtain precisely the same results. Nevertheless, to zeroth-order, the neutrino mechanism seems to work; therefore, one is tempted to declare that the overall problem of the mechanism of supernova explosions is solved, with the rest being details. However, these details include the credible mapping of progenitor mass and properties to important observables, such as explosion energy, neutron-star mass, nucleosynthesis, morphology, pulsar kicks and spins, and magnetic field magnitudes and multipolarities. Chaos will complicate all this, as will remaining uncertainties in microphysics and numerics. Nevertheless, we are confident that core-collapse supernova theory has reached a milestone, from which it need never look back.

1. Chandrasekhar, S. *An Introduction to the Study of Stellar Structure* (Dover Publications, 1939).
2. O'Connor, E. et al. Global comparison of core-collapse supernova simulations in spherical symmetry. *J. Phys. G* **45**, 104001 (2018).
   One of the few group-to-group and code-to-code comparison papers in supernova theory.
3. Radice, D., Burrows, A., Vartanyan, D., Skinner, M. A. & Dolence, J. C. Electron-capture and low-mass iron-core-collapse supernovae: new neutrino-radiation-hydrodynamics simulations. *Astrophys. J.* **850**, 43 (2017).
4. Burrows, A., Vartanyan, D., Dolence, J. C., Skinner, M. A. & Radice, D. Crucial physical dependencies of the core-collapse supernova mechanism. *Space Sci. Rev.* **214**, 33 (2018).
5. Vartanyan, D., Burrows, A., Radice, D., Skinner, M. A. & Dolence, J. Revival of the fittest: exploding core-collapse supernovae from 12 to 25 $M_{\odot}$. *Mon. Not. R. Astron. Soc.* **477**, 3091–3108 (2018).
6. Vartanyan, D., Burrows, A., Radice, D., Skinner, M. A. & Dolence, J. A successful 3D core-collapse supernova explosion model. *Mon. Not. R. Astron. Soc.* **482**, 351–369 (2019).
7. Burrows, A., Radice, D. & Vartanyan, D. Three-dimensional supernova explosion simulations of 9-, 10-, 11-, 12-, and 13-$M_{\odot}$ stars. *Mon. Not. R. Astron. Soc.* **485**, 3153–3168 (2019).
8. Nagakura, H., Burrows, A., Radice, D. & Vartanyan, D. Towards an understanding of the resolution dependence of core-collapse supernova simulations. *Mon. Not. R. Astron. Soc.* **490**, 4622–4637 (2019).
9. Burrows, A. et al. The overarching framework of core-collapse supernova explosions as revealed by 3D FORNAX simulations. *Mon. Not. R. Astron. Soc.* **491**, 2715–2735 (2020).
   The largest collection of full-physics 3D simulations published so far, describing the witnessed systematics with progenitor mass and initial core density structure.
10. Nagakura, H., Burrows, A., Radice, D. & Vartanyan, D. A systematic study of proto-neutron star convection in three-dimensional core-collapse supernova simulations. *Mon. Not. R. Astron. Soc.* **492**, 5764–5779 (2020).
11. Skinner, M. A., Dolence, J. C., Burrows, A., Radice, D. & Vartanyan, D. FORNAX: a flexible code for multiphysics astrophysical simulations. *Astrophys. J. Suppl. Ser.* **241**, 7 (2019).
12. Lentz, E. J. et al. Three-dimensional core-collapse supernova simulated using a 15 $M_{\odot}$ progenitor. *Astrophys. J. Lett.* **807**, L31 (2015).
    A comprehensive study of the hydrodynamics of a 3D core-collapse simulation.
13. Melson, T. et al. Neutrino-driven explosion of a 20 solar-mass star in three dimensions enabled by strange-quark contributions to neutrino–nucleon scattering. *Astrophys. J. Lett.* **808**, L42 (2015).
14. Melson, T., Janka, H.-T. & Marek, A. Neutrino-driven supernova of a low-mass iron-core progenitor boosted by three-dimensional turbulent convection. *Astrophys. J.* **801**, L24 (2015).
15. Janka, H.-T., Melson, T. & Summa, A. Physics of core-collapse supernovae in three dimensions: a sneak preview. *Annu. Rev. Nucl. Part. Sci.* **66**, 341–375 (2016).
    A useful review of core-collapse systematics, with some insights into the possible effects of rapid rotation.
16. Takiwaki, T., Kotake, K. & Suwa, Y. Three-dimensional simulations of rapidly rotating core-collapse supernovae: finding a neutrino-powered explosion aided by non-axisymmetric flows. *Mon. Not. R. Astron. Soc.* **461**, L112–L116 (2016).
17. Müller, B., Melson, T., Heger, A. & Janka, H.-T. Supernova simulations from a 3D progenitor model – impact of perturbations and evolution of explosion properties. *Mon. Not. R. Astron. Soc.* **472**, 491–513 (2017).
    An important paper on the potential effects of initial perturbations on supernova explosions.
18. O'Connor, E. P. & Couch, S. M. Exploring fundamentally three-dimensional phenomena in high-fidelity simulations of core-collapse supernovae. *Astrophys. J.* **865**, 81 (2018).
19. Kuroda, T., Kotake, K., Takiwaki, T. & Thielemann, F.-K. A full general relativistic neutrino radiation-hydrodynamics simulation of a collapsing very massive star and the formation of a black hole. *Mon. Not. R. Astron. Soc.* **477**, L80–L84 (2018).
    An important study using a fully general-relativistic hydrodynamic and transport approach.
20. Glas, R., Just, O., Janka, H. T. & Obergaulinger, M. Three-dimensional core-collapse supernova simulations with multidimensional neutrino transport compared to the ray-by-ray-plus approximation. *Astrophys. J.* **873**, 45 (2019).
21. Kuroda, T., Arcones, A., Takiwaki, T. & Kotake, K. Magnetorotational explosion of a massive star supported by neutrino heating in general relativistic three-dimensional simulations. *Astrophys. J.* **896**, 102 (2020).
22. Jones, S. et al. Do electron-capture supernovae make neutron stars? First multidimensional hydrodynamic simulations of the oxygen deflagration. *Astron. Astrophys.* **593**, A72 (2016).
23. Kirsebom, O. S. et al. Discovery of an exceptionally strong β-decay transition of ^{20}F and implications for the fate of intermediate-mass stars. *Phys. Rev. Lett.* **123**, 262701 (2019).
24. Jones, S. et al. Remnants and ejecta of thermonuclear electron-capture supernovae. Constraining oxygen-neon deflagrations in high-density white dwarfs. *Astron. Astrophys.* **622**, A74 (2019).
25. Zha, S., Leung, S.-C., Suzuki, T. & Nomoto, K. Evolution of ONeMg core in super-AGB stars toward electron-capture supernovae: effects of updated electron-capture rate. *Astrophys. J.* **886**, 22 (2019).
26. Burrows, A., Dessart, L., Livne, E., Ott, C. D. & Murphy, J. Simulations of magnetically driven supernova and hypernova explosions in the context of rapid rotation. *Astrophys. J.* **664**, 416–434 (2007).
    A magneto-radiation-hydrodynamic study of magnetic jet-driven explosions for rapidly rotating cores.
27. Mösta, P. et al. A large-scale dynamo and magnetoturbulence in rapidly rotating core-collapse supernovae. *Nature* **528**, 376–379 (2015).
28. Bethe, H. A. Supernova mechanisms. *Rev. Mod. Phys.* **62**, 801–866 (1990).
    An early qualitative discussion of the salient aspects of the delayed neutrino-driven explosion mechanism.
29. Woosley, S. & Janka, T. The physics of core-collapse supernovae. *Nat. Phys.* **1**, 147–154 (2005).
30. Janka, H.-T. Explosion mechanisms of core-collapse supernovae. *Annu. Rev. Nucl. Part. Sci.* **62**, 407–451 (2012).
    An important review of general core-collapse supernova physics.
31. Burrows, A. Perspectives on core-collapse supernova theory. *Rev. Mod. Phys.* **85**, 245–261 (2013).
32. Nomoto, K. Evolution of 8–10 solar mass stars toward electron capture supernovae. I – Formation of electron-degenerate O + Ne + Mg cores. *Astrophys. J.* **277**, 791–805 (1984).
33. Kitaura, F. S., Janka, H.-T. & Hillebrandt, W. Explosions of O-Ne-Mg cores, the Crab supernova, and subluminous type II-P supernovae. *Astron. Astrophys.* **450**, 345–350 (2006).
34. Burrows, A., Hayes, J. & Fryxell, B. A. On the nature of core-collapse supernova explosions. *Astrophys. J.* **450**, 830 (1995).
    One of the early papers detailing the role of convection and turbulence in the supernova explosion mechanism.
35. Foglizzo, T., Scheck, L. & Janka, H. T. Neutrino-driven convection versus advection in core-collapse supernovae. *Astrophys. J.* **652**, 1436–1450 (2006).
36. Chatzopoulos, E., Graziani, C. & Couch, S. M. Characterizing the convective velocity fields in massive stars. *Astrophys. J.* **795**, 92 (2014).
37. Couch, S. M. & Ott, C. D. The role of turbulence in neutrino-driven core-collapse supernova explosions. *Astrophys. J.* **799**, 5 (2015).
38. Müller, B. & Janka, H.-T. Non-radial instabilities and progenitor asphericities in core-collapse supernovae. *Mon. Not. R. Astron. Soc.* **448**, 2141–2174 (2015).
39. Murphy, J. W. & Burrows, A. Criteria for core-collapse supernova explosions by the neutrino mechanism. *Astrophys. J.* **688**, 1159–1175 (2008).
40. Müller, B. & Varma, V. A 3D simulation of a neutrino-driven supernova explosion aided by convection and magnetic fields. *Mon. Not. R. Astron. Soc.* **498**, L109–L113 (2020).
41. Burrows, A. & Sawyer, R. F. Effects of correlations on neutrino opacities in nuclear matter. *Phys. Rev. C* **58**, 554–571 (1998).

42. Burrows, A. & Sawyer, R. F. Many-body corrections to charged-current neutrino absorption rates in nuclear matter. *Phys. Rev. C* **59**, 510–514 (1999).
43. Reddy, S., Prakash, M., Lattimer, J. M. & Pons, J. A. Effects of strong and electromagnetic correlations on neutrino interactions in dense matter. *Phys. Rev. C* **59**, 2888–2918 (1999).
44. Burrows, A., Reddy, S. & Thompson, T. A. Neutrino opacities in nuclear matter. *Nucl. Phys. A* **777**, 356–394 (2006).
45. Roberts, L. F., Reddy, S. & Shen, G. Medium modification of the charged-current neutrino opacity and its implications. *Phys. Rev. C* **86**, 065803 (2012).
46. Fischer, T. et al. Neutrino signal from proto-neutron star evolution: effects of opacities from charged-current–neutrino interactions and inverse neutron decay. *Phys. Rev. C* **101**, 025804 (2020).
47. Roberts, L. F. & Reddy, S. Charged current neutrino interactions in hot and dense matter. *Phys. Rev. C* **95**, 045807 (2017).
48. Horowitz, C. J., Caballero, O. L., Lin, Z., O'Connor, E. & Schwenk, A. Neutrino–nucleon scattering in supernova matter from the virial expansion. *Phys. Rev. C* **95**, 025801 (2017).
49. Langanke, K. et al. Electron capture rates on nuclei and implications for stellar core collapse. *Phys. Rev. Lett.* **90**, 241102 (2003).
50. Juodagalvis, A., Langanke, K., Hix, W. R., Martínez-Pinedo, G. & Sampaio, J. M. Improved estimate of electron capture rates on nuclei during stellar core collapse. *Nucl. Phys. A* **848**, 454–478 (2010).
51. Lentz, E. J., Mezzacappa, A., Messer, O. E. B., Hix, W. R. & Bruenn, S. W. Interplay of neutrino opacities in core-collapse supernova simulations. *Astrophys. J.* **760**, 94 (2012).
52. Mezzacappa, A. & Bruenn, S. W. Stellar core collapse: a Boltzmann treatment of neutrino–electron scattering. *Astrophys. J.* **410**, 740 (1993).
53. Bruenn, S. W. et al. CHIMERA: a massively parallel code for core-collapse supernova simulations. *Astrophys. J. Suppl. Ser.* **248**, 11 (2020).
54. Dolence, J. C., Burrows, A., Murphy, J. W. & Nordhaus, J. Dimensional dependence of the hydrodynamics of core-collapse supernovae. *Astrophys. J.* **765**, 110 (2013).
55. Vartanyan, D., Burrows, A. & Radice, D. Temporal and angular variations of 3D core-collapse supernova emissions and their physical correlations. *Mon. Not. R. Astron. Soc.* **489**, 2227–2246 (2019).
56. Couch, S. M., Chatzopoulos, E., Arnett, W. D. & Timmes, F. X. The three-dimensional evolution to core collapse of a massive star. *Astrophys. J.* **808**, L21 (2015).
A benchmark study of 3D stellar evolution just prior to core collapse.
57. Chatzopoulos, E., Couch, S. M., Arnett, W. D. & Timmes, F. X. Convective properties of rotating two-dimensional core-collapse supernova progenitors. *Astrophys. J.* **822**, 61 (2016).
58. Müller, B. et al. Three-dimensional simulations of neutrino-driven core-collapse supernovae from low-mass single and binary star progenitors. *Mon. Not. R. Astron. Soc.* **484**, 3307–3324 (2019).
59. Keil, W., Janka, H.-T. & Mueller, E. Ledoux convection in protoneutron stars—a clue to supernova nucleosynthesis? *Astrophys. J.* **473**, L111 (1996).
60. Dessart, L., Burrows, A., Livne, E. & Ott, C. D. Multidimensional radiation/hydrodynamic simulations of proto-neutron star convection. *Astrophys. J.* **645**, 534–550 (2006).
61. Sukhbold, T., Woosley, S. E. & Heger, A. A high-resolution study of presupernova core structure. *Astrophys. J.* **860**, 93 (2018).
An important source of 1D massive star progenitor models using a state-of-the-art stellar evolution code.
62. O'Connor, E. & Ott, C. D. Black hole formation in failing core-collapse supernovae. *Astrophys. J.* **730**, 70 (2011).
63. Ebinger, K. et al. PUSHing core-collapse supernovae to explosions in spherical symmetry. IV. Explodability, remnant properties, and nucleosynthesis yields of low-metallicity stars. *Astrophys. J.* **888**, 91 (2020).
64. Müller, B. The dynamics of neutrino-driven supernova explosions after shock revival in 2D and 3D. *Mon. Not. R. Astron. Soc.* **453**, 287–310 (2015).
65. Hanke, F., Marek, A., Müller, B. & Janka, H.-T. Is strong SASI activity the key to successful neutrino-driven supernova explosions? *Astrophys. J.* **755**, 138 (2012).
66. Hanke, F., Müller, B., Wongwathanarat, A., Marek, A. & Janka, H.-T. SASI activity in three-dimensional neutrino-hydrodynamics simulations of supernova cores. *Astrophys. J.* **770**, 66 (2013).
67. Couch, S. M. On the impact of three dimensions in simulations of neutrino-driven core-collapse supernova explosions. *Astrophys. J.* **775**, 35 (2013).
68. Summa, A. et al. Progenitor-dependent explosion dynamics in self-consistent, axisymmetric simulations of neutrino-driven core-collapse supernovae. *Astrophys. J.* **825**, 6 (2016).
69. Summa, A., Janka, H.-T., Melson, T. & Marek, A. Rotation-supported neutrino-driven supernova explosions in three dimensions and the critical luminosity condition. *Astrophys. J.* **852**, 28 (2018).
70. Sukhbold, T., Ertl, T., Woosley, S. E., Brown, J. M. & Janka, H.-T. Core-collapse supernovae from 9 to 120 solar masses based on neutrino-powered explosions. *Astrophys. J.* **821**, 38 (2016).
71. Ertl, T., Woosley, S. E., Sukhbold, T. & Janka, H. T. The explosion of helium stars evolved with mass loss. *Astrophys. J.* **890**, 51 (2020).
72. Özel, F., Psaltis, D., Narayan, R. & Santos Villarreal, A. On the mass distribution and birth masses of neutron stars. *Astrophys. J.* **757**, 55 (2012).
73. Pruet, J., Hoffman, R. D., Woosley, S. E., Janka, H. T. & Buras, R. Nucleosynthesis in early supernova winds. II. The role of neutrinos. *Astrophys. J.* **644**, 1028–1039 (2006).
74. Fröhlich, C. et al. Neutrino-induced nucleosynthesis of $A > 64$ nuclei: the *vp* process. *Phys. Rev. Lett.* **96**, 142502 (2006).
75. Fischer, T., Whitehouse, S. C., Mezzacappa, A., Thielemann, F.-K. & Liebendörfer, M. Protoneutron star evolution and the neutrino-driven wind in general relativistic neutrino radiation hydrodynamics simulations. *Astron. Astrophys.* **517**, A80 (2010).
76. Thielemann, F.-K., Hashimoto, M.-A. & Nomoto, K. Explosive nucleosynthesis in SN 1987A. II. Composition, radioactivities, and the neutron star mass. *Astrophys. J.* **349**, 222 (1990).
77. Tamborra, I. et al. Self-sustained asymmetry of lepton-number emission: a new phenomenon during the supernova shock-accretion phase in three dimensions. *Astrophys. J.* **792**, 96 (2014).
78. Glas, R., Janka, H. T., Melson, T., Stockinger, G. & Just, O. Effects of LESA in three-dimensional supernova simulations with multidimensional and ray-by-ray-plus neutrino transport. *Astrophys. J.* **881**, 36 (2019).
79. Arzoumanian, Z., Chernoff, D. F. & Cordes, J. M. The velocity distribution of isolated radio pulsars. *Astrophys. J.* **568**, 289–301 (2002).
80. Faucher-Giguère, C.-A. & Kaspi, V. M. Birth and evolution of isolated radio pulsars. *Astrophys. J.* **643**, 332–355 (2006).
81. Cordes, J. M., Romani, R. W. & Lundgren, S. C. The Guitar nebula: a bow shock from a slow-spin, high-velocity neutron star. *Nature* **362**, 133–135 (1993).
82. Burrows, A. & Hayes, J. Pulsar recoil and gravitational radiation due to asymmetrical stellar collapse and explosion. *Phys. Rev. Lett.* **76**, 352–355 (1996).
83. Scheck, L., Plewa, T., Janka, H. T., Kifonidis, K. & Müller, E. Pulsar recoil by large-scale anisotropies in supernova explosions. *Phys. Rev. Lett.* **92**, 011103 (2004).
A summary of general theory and results concerning the recoil mechanism of pulsar kick speeds.
84. Scheck, L., Kifonidis, K., Janka, H. T. & Müller, E. Multidimensional supernova simulations with approximative neutrino transport. I. Neutron star kicks and the anisotropy of neutrino-driven explosions in two spatial dimensions. *Astron. Astrophys.* **457**, 963–986 (2006).
85. Wongwathanarat, A., Janka, H.-T. & Müller, E. Hydrodynamical neutron star kicks in three dimensions. *Astrophys. J.* **725**, L106–L110 (2010).
86. Nordhaus, J., Brandt, T. D., Burrows, A. & Almgren, A. The hydrodynamic origin of neutron star kicks. *Mon. Not. R. Astron. Soc.* **423**, 1805–1812 (2012).
87. Wongwathanarat, A., Janka, H. T. & Müller, E. Three-dimensional neutrino-driven supernovae: neutron star kicks, spins, and asymmetric ejection of nucleosynthesis products. *Astron. Astrophys.* **552**, A126 (2013).
88. Nakamura, K., Takiwaki, T. & Kotake, K. Long-term simulations of multi-dimensional core-collapse supernovae: implications for neutron star kicks. *Publ. Astron. Soc. Jpn.* **71**, 98 (2019).
89. Burrows, A., Livne, E., Dessart, L., Ott, C. D. & Murphy, J. Features of the acoustic mechanism of core-collapse supernova explosions. *Astrophys. J.* **655**, 416–433 (2007).
90. Burrows, A. The birth of neutron stars and black holes. *Phys. Today* **40**, 28–37 (1987).
91. Timmes, F. X., Woosley, S. E. & Weaver, T. A. The neutron star and black hole initial mass function. *Astrophys. J.* **457**, 834 (1996).
92. Chan, C., Müller, B., Heger, A., Pakmor, R. & Springel, V. Black hole formation and fallback during the supernova explosion of a 40 $M_{\odot}$ star. *Astrophys. J. Lett.* **852**, 19 (2018).
93. Woosley, S., Sukhbold, T. & Janka, H. T. The birth function for black holes and neutron stars in close binaries. *Astrophys. J.* **896**, 56 (2020).
94. Farr, W. M. et al. The mass distribution of stellar-mass black holes. *Astrophys. J.* **741**, 103 (2011).
95. Seadrow, S., Burrows, A., Vartanyan, D., Radice, D. & Skinner, M. A. Neutrino signals of core-collapse supernovae in underground detectors. *Mon. Not. R. Astron. Soc.* **480**, 4710–4731 (2018).
96. Cerdá-Durán, P., DeBrye, N., Aloy, M. A., Font, J. A. & Obergaulinger, M. Gravitational wave signatures in black hole forming core collapse. *Astrophys. J.* **779**, L18 (2013).
97. Burrows, A. Speculations on the fizzled collapse of a massive star. *Astrophys. J.* **300**, 488 (1986).
98. Nadyozhin, D. K. Some secondary indications of gravitational collapse. *Astrophys. Space Sci.* **69**, 115–125 (1980).
99. Lovegrove, E. & Woosley, S. E. Very low energy supernovae from neutrino mass loss. *Astrophys. J.* **769**, 109 (2013).
100. Blondin, J. M. & Mezzacappa, A. Pulsar spins from an instability in the accretion shock of supernovae. *Nature* **445**, 58–60 (2007).
101. Rantsiou, E., Burrows, A., Nordhaus, J. & Almgren, A. Induced rotation in three-dimensional simulations of core-collapse supernovae: implications for pulsar spins. *Astrophys. J.* **732**, 57 (2011).
102. Stockinger, G. et al. Three-dimensional models of core-collapse supernovae from low-mass progenitors with implications for Crab. *Mon. Not. R. Astron. Soc.* **496**, 2039–2084 (2020).
103. Morozova, V., Piro, A. L. & Valenti, S. Measuring the progenitor masses and dense circumstellar material of Type II supernovae. *Astrophys. J.* **858**, 15 (2018).
104. Martinez, L. & Bersten, M. C. Mass discrepancy analysis for a select sample of Type II-plateau supernovae. *Astron. Astrophys.* **629**, A124 (2019).
105. Pumo, M. L. & Zampieri, L. Radiation-hydrodynamical modeling of core-collapse supernovae: light curves and the evolution of photospheric velocity and temperature. *Astrophys. J.* **741**, 41 (2011).
106. Pumo, M. L. et al. Radiation-hydrodynamical modelling of underluminous Type II plateau supernovae. *Mon. Not. R. Astron. Soc.* **464**, 3013–3020 (2017).
107. Utrobin, V. P. Nonthermal ionization and excitation in Type IIb supernova 1993J. *Astron. Astrophys.* **306**, 219 (1996).
108. Utrobin, V. P. & Chugai, N. N. Type IIP supernova 2008in: the explosion of a normal red supergiant. *Astron. Astrophys.* **555**, A145 (2013).
109. Utrobin, V. P. & Chugai, N. N. Luminous Type IIP SN 2013ej with high-velocity ^{56}Ni ejecta. *Mon. Not. R. Astron. Soc.* **472**, 5004–5010 (2017).
110. Utrobin, V. P. & Chugai, N. N. Resolving the puzzle of type IIP SN 2016X. *Mon. Not. R. Astron. Soc.* **490**, 2042–2049 (2019).

Acknowledgements We thank J. Insley and S. Rizzi of the Argonne National Laboratory and the Argonne Leadership Computing Facility (ALCF) for considerable support with the 3D graphics. We also acknowledge ongoing collaborations with H. Nagakura, D. Radice, J. Dolence, A. Skinner and M. Coleman. We acknowledge E. O'Connor regarding the equation of state, G. Martínez-Pinedo concerning electron capture on heavy nuclei, T. Sukhbold and S. Woosley for providing details concerning the initial models, and T. Thompson and T. Wang regarding inelastic scattering. Funding was provided by the US Department of Energy (DOE) Office of Science and the Office of Advanced Scientific Computing Research via the Scientific Discovery through Advanced Computing (SciDAC4) programme and Grant DE-SC0018297 (subaward 00009650) and by the US NSF under grants AST-1714267 and PHY-1804048 (the

latter via the Max-Planck/Princeton Center (MPPC) for Plasma Physics). Awards of computer time were provided by the INCITE programme using resources of the ALCF, which is a DOE Office of Science User Facility supported under Contract DE-AC02-06CH11357, under a Blue Waters sustained-petascale computing project, supported by the National Science Foundation (awards OCI-0725070 and ACI-1238993) and the state of Illinois, under a PRAC allocation from the National Science Foundation (#OAC-1809073), and under award #TG-AST170045 to the resource Stampede2 in the Extreme Science and Engineering Discovery Environment (XSEDE, ACI-1548562). Finally, we employed computational resources provided by the TIGRESS high-performance computer centre at Princeton University, which is jointly supported by the Princeton Institute for Computational Science and Engineering (PICSciE) and the Princeton University Office of Information Technology, and acknowledge their continuing allocation at the National Energy Research Scientific Computing Center (NERSC), supported by the DOE Office of Science under contract DE-AC03-76SF00098.

Author contributions A.B. organized the paper and wrote most of it. D.V. conducted the 2D calculations. Otherwise, the authors contributed equally to the document.

Competing interests The authors declare no competing interests.

Additional information
Correspondence and requests for materials should be addressed to A.B.
Peer review information *Nature* thanks Friedrich-Karl Thielemann and Stan Woosley for their contribution to the peer review of this work.
Reprints and permissions information is available at http://www.nature.com/reprints.
Publisher's note Springer Nature remains neutral with regard to jurisdictional claims in published maps and institutional affiliations.